IFSCC 2025 full paper (IFSCC2025-1157)

Enzymatically Hydrolyzed Peony Seed Peptides: A Comprehensive Study From Anti-Aging Activity to Molecular Mechanisms

Rong Tang* [1], Meijin Li[1], Na Yang[1], Xichao Fu[1], Yunpeng Dong[1], Dan Liu[1], Meng Wang[1], Zichen Liu[1], Xiaolin Tang[1], Minhua Hong[1]

[1] Shanghai Peptide Biotechnology Co., Ltd, Shanghai, 201708, China

Abstract

1. Introduction

Plant protein-derived active peptides, due to their eco-friendly, efficient, and safe advantages, have gradually emerged as alternative anti-aging ingredients to animal-derived active peptides. However, comprehensive studies on the development and molecular mechanisms of plant-derived active peptides remain relatively scarce, limiting their extensive application in the cosmetics industry. Therefore, this study employs enzymatic hydrolysis technology to develop peony seed meal peptides (PSMPs) — also referred to as peony seed peptides — with high anti-aging efficacy. Additionally, Quantitative Gene Plex (QGP) gene testing, LC-MS/MS, De Novo and molecular docking are used to further elucidate its potential molecular mechanisms of action.

2. Methods

The anti-aging effect of PSMPs was evaluated by measuring antioxidant indices (DPPH·, ABTS+·, O_2^-·, etc.) and conducting human fibroblast experiments (MMP-1, ROS, type I collagen, etc.). In addition, the QGP gene testing technique was employed to explore the molecular regulatory mechanisms of PSMPs on a variety of genes related to antioxidant, anti-aging, and

anti-inflammatory pathways. LC-MS/MS combined with De Novo sequencing was used to analyze the peptide sequences within PSMPs. Finally, potential anti-aging peptides were identified through a dual-screening strategy combining Peptide Ranker and molecular docking. The screening criteria were as follows: For Peptide Ranker, a score > 0.8 was required. For molecular docking, the selected targets were MMP-1 and elastase, which are representative enzymes related to aging, with a binding energy (ΔG) < -5 kcal/mol. Peptides that satisfied both criteria were considered to have potential anti-aging effects.

3. Results

The PSMPs demonstrated significant antioxidant effects across all of the above indicators. At low concentrations, they exhibited the ability to promote type I, VII collagen production and inhibit ROS levels. Among them, the inhibitory effects on MMP-1 and MMP-3 were superior to those of the PC group (VC+VE=100 μg/mL). QGP results showed that the PSMPs can regulate the NF-κB/NFR2 and NF-κB/AMPK pathways, thereby exerting their anti-aging effects. Based on the LC-MS/MS and De Novo sequencing results, and through a dual screening strategy combining Peptide Ranker scoring and molecular docking, ten potential peptides with possible anti-aging effects were identified from PSMPs.

4. Conclusion

Peony seed peptides exhibit multiple anti-aging effects by regulating two key signaling pathways: NF-κB/NRF2 and NF-κB/AMPK, thereby exerting antioxidant and anti-photoaging activities. Furthermore, LC-MS/MS and De Novo sequencing were employed to preliminarily identify the peptide sequences in PSMPs. Through a dual screening strategy combining Peptide Ranker scoring and molecular docking, ten core peptides with potential anti-aging functions were identified. This study provides strong support for the application of peony seed meal peptides as a natural anti-aging ingredient in skincare and anti-aging fields.

1. Introduction

As the global population continues to age at an accelerating pace, the demand for anti-aging skincare products is steadily increasing. However, mainstream anti-aging ingredients currently in use exhibit certain limitations. For example, vitamin derivatives such as retinol are

susceptible to oxidative degradation, whereas compounds like ergothioneine involve high production costs. Additionally, traditional antioxidants, such as vitamin E, demonstrate relatively limited efficacy. Furthermore, most of these ingredients rely on unsustainable chemical synthesis processes. Consequently, the development of next-generation anti-aging ingredients that are efficacious, economically viable, and environmentally sustainable is crucial for facilitating the green transition and long-term sustainability of the cosmetics industry.

Literature indicates that plant proteins possess high biocompatibility, wide availability, and environmental friendliness, showing great potential for development and application in the anti-aging field [1]. Currently, the application of plant proteins in skincare products is mostly focused on moisturization and barrier repair [2], while systematic research on their anti-aging effects remains limited. Peony seed meal, as an oil processing byproduct, is rich in high-quality proteins (>20%) and antioxidant components, making it an ideal raw material for anti-aging development [3]. Based on this, we successfully developed peptides with potent anti-aging effects — peony seed meal peptides (PSMPs), also referred to as peony seed peptides — using a mild and efficient enzymatic hydrolysis technique. Its anti-aging activity was validated through relevant antioxidant assays and photodamage cellular experiments. Additionally, advanced techniques, such as Quantitative Gene Plex (QGP) gene testing, LC-MS/MS, and molecular docking, were employed to further reveal its molecular mechanisms and potential active ingredients. This study aims to provide a theoretical foundation and scientific basis for the innovative application of plant proteins in the anti-aging field.

2. Materials and Methods

Materials

DPPH, ABTS, Anhydrous ethanol, Pyrogallol, $FeSO_4 \cdot 4H_2O$, Potassium ferrocyanide, $FeCl_3$ and other reagents was purchased from Sinopharm Chemical Reagent Co., Ltd. (Shanghai，China). Ferrozine, TCA, Tris-HCl and other reagents was purchased from Macklin Biochemical Co., Ltd. (Shanghai, China).The human foreskin fibroblasts (HFF) was sourced from the Institute of Stem Cell Research, Chinese Academy of Sciences (Beijing, China). The DMSO,Type I collagen,Type VII collagen, human MMP-1, MMP-3 ELISA kits, and other

reagents were purchased from Sigma-Aldrich Co., Ltd. (Merck, Germany). Vitamin C and vitamin E were obtained from Aladdin Biochemical Technology Co., Ltd. (Shanghai, China). QuantiGene™ Plex Assay Kit, formic acid and acetonitrile were purchased from Fisher Scientific. (Waltham, MA, USA). All reagents were of analytical grade.

Methods

DPPH·, $ABTS^{+}$·, O_2^{-}·, Fe^{2+}, FRAP antioxidant activity assay

DPPH · scavenging rate refers to the literature of Huang et al. with slight modifications [4]. Take 200 μ L of PSMPs solutions with concentrations of 1, 5, and 10 mg/mL and 0.1 mg/mL of VC solution (PC group), and mix them with 200 μ L, Mix 200 μg/mL DPPH · solution, let it stand for 20 minutes, and measure its OD value at 517 nm using a spectrophotometer (SpectraMax iD3, Molecular Devices, LLC, San Jose, CA, USA). (A) Sample group; (A1) Sample control group; (A0) Blank group. The formula for calculating DPPH clearance rate is as follows:

$$\text{DPPH} \cdot \text{ scavenging rate}(\%)=\left(1-\frac{A-A_1}{A_0}\right)\times 100\% \quad (1)$$

The $ABTS^{+}$· scavenging rate, O_2^{-}· scavenging rate, and Fe^{2+} chelating ability were determined according to the methods described by Jia et al. [5], Liu et al. [6], and Duan et al. [7], respectively, with slight modifications. For all assays, the sample concentrations (1, 5, and 10 mg/mL PSMPs solutions and 0.1 mg/mL ascorbic acid as positive control) and calculation formulas were consistent with those used in the DPPH· scavenging rate determination.

The $ABTS^{+}$· solution was generated by reacting 7 mmol/L ABTS with 2.45 mmol/L potassium persulfate (1:1, v/v) for 24 h in the dark. After adjusting the $OD_{734\ nm}$ to 0.70 ± 0.02 with 95% ethanol, 0.4 mL of samples were mixed with 3.6 mL $ABTS^{+}$· solution. After 5 min of dark incubation, absorbance was recorded at 734 nm.

The O_2^{-}·scavenging rate was determined by mixing 0.2 mL of sample with 1 mL of 50 mmol/L Tris-HCl buffer (pH 8.2). After incubation at 25 °C for 10 min, 30 μL of 6 mmol/L pyrogallol was added. The reaction proceeded at room temperature for 8 min, and absorbance was recorded at 320 nm.

The Fe^{2+} chelating rate was evaluated by reacting 100 μL of sample with 100 μL of 1.3

mmol/L $FeCl_2 \cdot 4H_2O$ for 30 min at 25 °C. Subsequently, 50 μL of 0.1 mmol/L Ferrozine solution was added, and absorbance was measured at 562 nm after 10 min equilibrium.

The ferric reducing antioxidant power (FRAP) refers to the literature of Yousuf et al. with slight modifications [8]. Mix 250 μL of sample with 250 μL of potassium ferrocyanide (1%) solution, keep at 50 ℃ for 20 minutes, then add 250 μL of 10% TCA aqueous solution and mix. Centrifuge for 10 minutes using a centrifuge(5415R, Eppendorf AG, Hamburg, Germany). Take 100 μL of supernatant and mix it with 20 μL, 0.1% $FeCl_3$ aqueous solution, and 80 μL distilled water. Let it stand at room temperature for 10 minutes, and measure its OD value at 700 nm using an enzyme-linked immunosorbent assay (ELISA) reader.(A) Sample group; (A_1) Sample control group; (A_0) Blank group. The formula for calculating DPPH clearance rate is as follows:

$$\text{FRAP(A700nm)}=(A-A_1-A_0) \quad (2)$$

Type I collagen, Type VII collagen, MMP-1, MMP-3, ROS assay

HFF cells are seeded in 24-well plates at a density that achieves 45-60% confluence after 24 hours, and incubated overnight in a CO_2 incubator (NU-850, Thermo Fisher Scientific Inc., Waltham, MA, USA). After UVA irradiation at a dose of 9 J/cm², the cells are divided into the following treatment groups: Sample group: PSMPs at concentrations of 0.1, 0.01, and 0.001 mg/mL (within the safe concentration range); PC group: 100 μg/mL VC + 7 μg/mL VE; NC group: no treatment; BC group: cells are treated with culture medium and covered with aluminum foil to avoid UV exposure. After 24 hours of incubation, collect the cell culture supernatants from each group and store them in a -80°C ultra-low temperature freezer (UXF40086A, Thermo Fisher Scientific Inc., Waltham, MA, USA) for future analysis. The levels of Type I collagen, Type VII collagen, MMP-1, and MMP-3 are measured according to the instructions provided by the ELISA kit.

The cell culture method is the same as described above. After incubation, the cells are divided into treatment groups. Sample group: PSMPs at concentrations of 0.1, 0.01, and 0.001 mg/mL; PC group: 0.05% VE; NC group and BC group: culture medium added; incubate for 24 hours. After incubation, all groups except the blank control group undergo H_2O_2 induction.

The cell culture supernatants are collected. Then, 1 mL of diluted 10 μmol/L DCFH-DA probe is added to each well and incubated at 37°C in the cell incubator. After 30 minutes, the cells are washed with PBS to thoroughly remove any probe that did not enter the cells. Fluorescence microscopy is used to take images at an excitation wavelength of 488 nm, and ROS fluorescence intensity is measured.

Quantitative Gene Plex (QGP) assay

The cell culture method is the same as described above. After incubation, the cells are divided into treatment groups. Sample group: 0.1 mg/mL PSMPs solution; NC group: culture medium added; after incubating for 18-22 hours, the cell culture supernatants are collected and stored at -80°C in a low-temperature freezer. The QGP operation steps follow the protocol described in the reference [9]. Finally, the detection and analysis are performed using the Luminex200 suspension bead array system (BIO-RAD, Bio-Plex PROTM, USA).

LC/MS/MS，De Novo identification

After desalting the samples, dissolve them in 20 μL of 0.1% formic acid, vortex thoroughly, centrifuge at 17,000 rpm for 20 minutes at 4°C, collect the supernatant, and take 4 μL of the supernatant for mass spectrometry analysis (1290 Infinity II, Agilent Technologies Inc., Santa Clara, CA, USA). The PEAKS software is used to search the database (https://www.bioinfor.com/peaks-studio/), and peptides that are not identified are analyzed using de novo sequencing.

Peptide Ranker screening

The peptide segments are scored using the Peptide Ranker website (http://distilldeep.ucd.ie/Peptide Ranker/), with scores >0.8 being used as the evaluation criterion for subsequent screening [10].

Molecular Docking

The 3D structures of MMP-1 (PDB ID: 966C) and Elastase (PDB ID: 1B0F) were obtained from the Protein Data Bank (PDB) database (https://pubchem.ncbi.nlm.nih.gov/) and processed as receptor proteins. PSMPs sequence structures were batch-generated using RDKit software (Version 2023.03.1) and preprocessed. High-precision 3D complex structures

were generated using AlphaFold3, and the binding modes between targets and peptides were preliminarily simulated. Molecular docking was performed using the Hermite® platform-Uni-Dock (https://hermite.dp.tech, DP Technology), and the docking results were visualized and analyzed using the Hermite® platform. For MMP-1, the docking center coordinates were set to (center_x = 12.86; center_y = -10.86; center_z = 36.88) with a grid map size of 20Å × 20Å × 20Å. For elastase, the docking center coordinates were (center_x = 64.59; center_y = 53.55; center_z = 56.86) with a grid map size of 25Å × 25Å × 25Å.Binding energy values of less than -5 kcal/mol were used as the evaluation criterion for subsequent screening.

Statistical analysis

GraphPad Prism 9.0 (GraphPad Software, Inc., La Jolla, CA, USA) was used for graphing and statistical data analysis. Significance testing was performed using ANOVA and t-tests. Statistical significance was defined as follows: ***$p < 0.001$, **$p < 0.01$, *$p < 0.05$, ##$p < 0.01$, #$p < 0.05$. Data are presented as mean ± standard deviation (Mean ± SD), and all experiments were repeated at least three times.

3. Results and Discussion

DPPH·, $ABTS^{+}$·, O_2^{-}·, Fe^{2+}, FRAP antioxidant activity assay

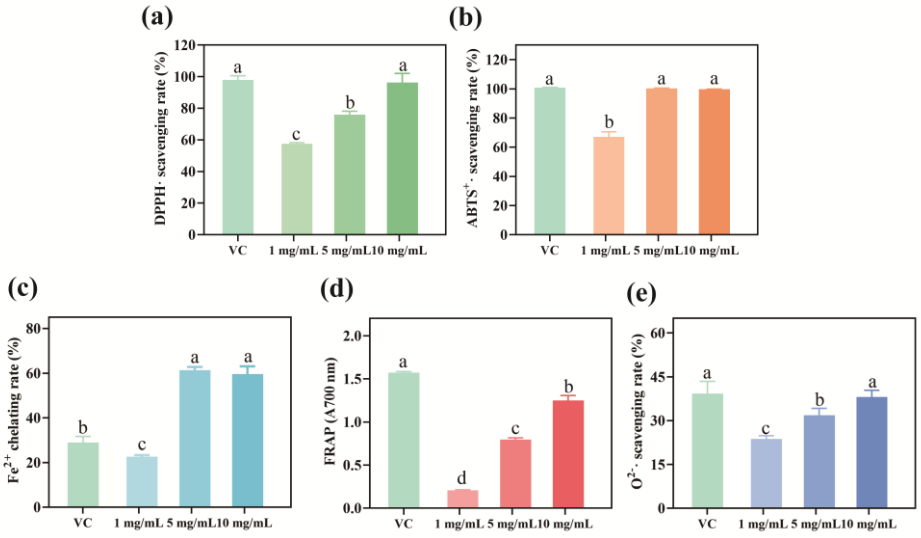

Figure 1. Evaluation of five antioxidant activities of PSMPs. (a) DPPH· scavenging rate. (b) $ABTS^{+}$· scavenging rate. (c) Fe^{2+} chelating ability. (d) FRAP (Ferric Reducing Antioxidant Power). (e) O_2^{-}· scavenging rate.Different lowercase letters indicate significant differences between groups ($p < 0.05$).

Antioxidant capacity is one of the key indicators for evaluating anti-aging activity.Samples can alleviate oxidative stress-induced damage to DNA, proteins, and other components in skin cells by scavenging excess free radicals, thereby delaying the skin aging process [11]. We systematically assessed the antioxidant capacity of PSMPs using five in vitro antioxidant assays, as shown in Figure 1(a–e).

The results indicate that PSMPs exhibit excellent antioxidant effects on the above indicators at various concentrations ($p < 0.5$). Specifically, the $ABTS^{+}\cdot$ scavenging rate of 5 mg/mL PSMPs is close to 100%, and its Fe^{2+} chelation ability is significantly superior to that of VC (PC group). At 10 mg/mL, PSMPs also nearly completely eliminate DPPH·, and at this concentration, the $O_2^{-}\cdot$ scavenging rate is not significantly different from that of VC ($p < 0.5$). In conclusion, PSMPs can exert potential effects in delaying skin oxidative damage and aging processes through multiple synergistic antioxidant mechanisms.

Type I collagen, Type VII collagen, MMP-1, MMP-3, ROS assay

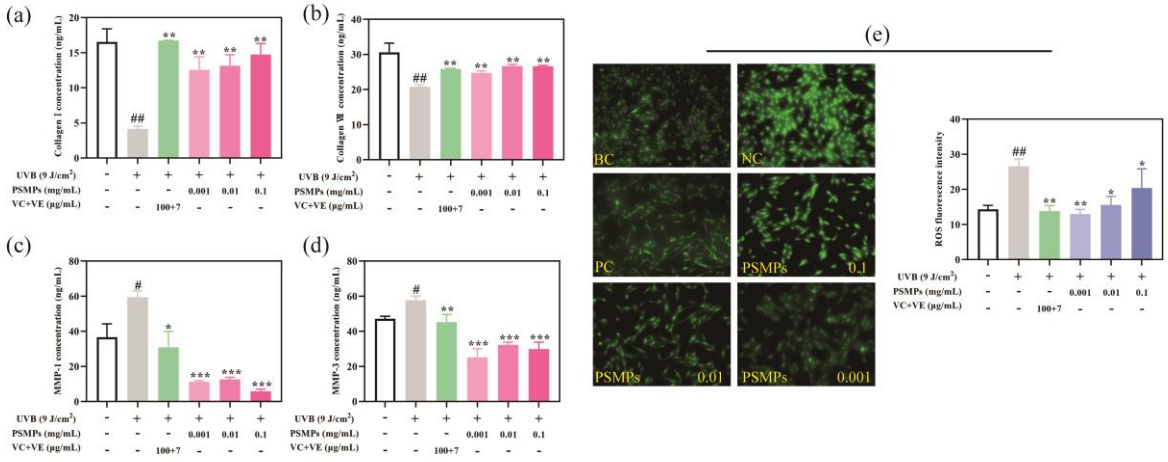

Figure 2. Evaluation of five anti-aging effects of PSMPs in HFF cells. (a) Type I collagen content. (b) Type VII collagen content. (c) MMP-1 content. (d) MMP-3 content. (e) ROS fluorescence intensity and representative fluorescence images. ***$p < 0.001$, **$p < 0.01$, *$p < 0.05$ indicate significant differences between different sample concentrations and the NC group. ##$p < 0.01$, #$p < 0.05$ indicate significant differences between the NC group and the BC group.

Type I and Type VII collagens are crucial components for maintaining skin structure and elasticity. UVB-induced photoaging impairs collagen synthesis and accelerates its degradation, thereby weakening the skin's support and elasticity. Meanwhile, key enzymes responsible for collagen degradation, such as MMP-1 and MMP-3, show increased activity during photoaging, further exacerbating skin aging. By measuring these critical indicators, the intervention effects of PSMPs on skin photoaging can be effectively evaluated [12].

The results shown in Figures (a–d) demonstrate that PSMPs exhibit significant effects on the above indicators (***$p < 0.001$, **$p < 0.01$, *$p < 0.05$), and notably, these effects are also significant at a low concentration of 0.001 mg/mL. It is worth noting that PSMPs exhibit stronger inhibitory effects on MMP-1 and MMP-3 than the PC group (VC + VE) across low, medium, and high concentrations.

Excessive accumulation of ROS can cause intracellular oxidative damage and accelerate the process of cellular aging [13]. Fluorescent probes typically exhibit low or no fluorescence when not interacting with ROS. The presence of ROS alters the chemical structure of the probe through an oxidation reaction, enhancing its fluorescence. Therefore, changes in fluorescence intensity can effectively reflect changes in ROS levels. A lower fluorescence intensity indicates that PSMPs can effectively reduce ROS production, thereby further inhibiting oxidative stress.

The results in Figure (e) show that the fluorescence intensity of the NC group significantly increased after UVB irradiation. Within the concentration range of 0.1-0.001 mg/mL, PSMPs significantly reduced the fluorescence intensity (**p <0.01, *p <0.05), particularly at the low concentration of 0.001 mg/mL, where the fluorescence intensity of PSMPs was not significantly different from the PC group, demonstrating excellent ROS scavenging ability. In summary, PSMPs exhibited significant effects in alleviating skin photoaging and have good free radical scavenging ability at the cellular level.

Quantitative Gene Plex (QGP) assay

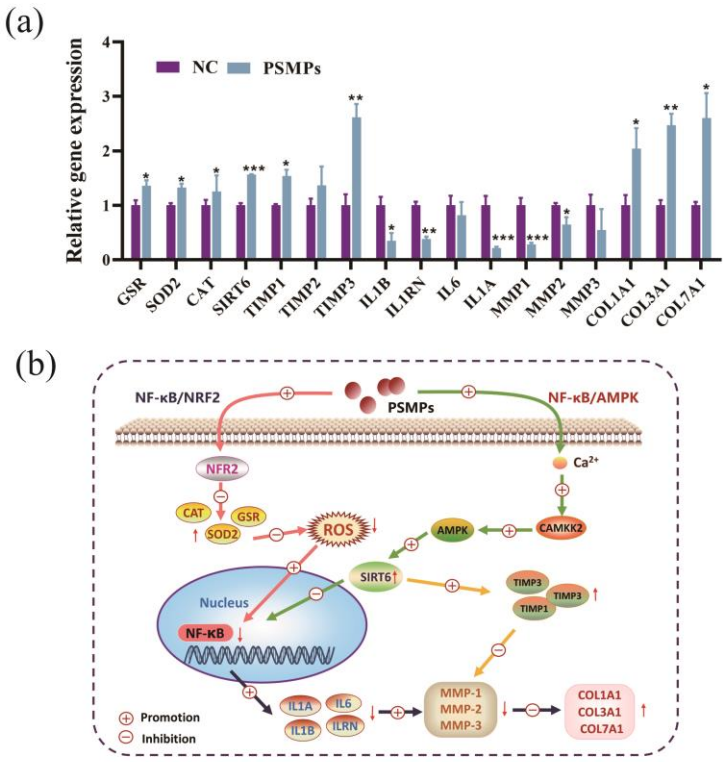

Figure 3. Effect of PSMPs on the gene expression of the NF-κB/NRF3 and NFκB/AMPK signaling pathways in HFF cells. (a) QGP detection of the relevant gene expression levels in HFF cells. (b) Diagram of the NF-κB/NRF3 and NF-κB/AMPK signaling pathways. ***p <0.001, **p <0.01, *p <0.05 indicate significant differences between different sample concentrations and the NC group.

To further analyze the mechanism by which PSMPs exert anti-aging effects, we employed QGP detection technology, which directly measures RNA transcription products through signal amplification, and combined it with microsphere dual-fluorescence labeling and flow dispersion laser detection technology to conduct high-throughput expression profile analysis of multi-target genes under PSMPs intervention. Aging is a complex biological process, and the theory of "inflammatory aging" has received widespread attention in recent years. The NF-κB signaling pathway, as an important regulatory mechanism of endogenous inflammatory responses, is considered one of the key pathways that induce inflammatory aging [14-15].

Based on the results from Figure 3 (a-b), we conclude that PSMPs primarily exert anti-aging effects through the NF-κB/NRF2 and NF-κB/AMPK pathways. In the NF-κB/AMPK

pathway, the Sirtuins family member SIRT6, recognized as a "longevity factor," plays a key role in delaying aging. PSMPs activate the expression of SIRT6, and SIRT6, through negative feedback regulation, inhibits the transcriptional activity of NF-κB, thereby reducing the expression of inflammatory factors such as IL-6, inhibiting the activity of matrix metalloproteinases like MMP-1, and upregulating the synthesis of collagen from the COL family. Additionally, in the NF-κB/NRF2 pathway, PSMPs promote the expression of antioxidant factors like CAT, enhance the cell's ability to clear ROS, reduce oxidative stress levels, and subsequently inhibit the transcriptional activity of NF-κB, downregulating the expression of inflammatory factors and related genes, ultimately exerting anti-aging effects.

LC/MS/MS，De Novo identification

Table 1. Hydrophobic amino acid > 60% peptide sequences of PSMPs selected from LC-MS/MS data.

Number	Peptide	-10LgP	Hydrophobic residues (%)	Accession
1	LXR	27.18	66%	A0A4P8VM05|A0A4P8VM05_9MAGN
2	YAL	26.98	66%	Q9GDR0|Q9GDR0_CHRAE
3	SXF	23.11	66%	A0A4P8VP44|A0A4P8VP44_9MAGN
4	RLI	27.67	66%	A6YA39|A6YA39_9MAGN
5	IXXXL	21.46	60%	Q9GI23|Q9GI23_9MAGN
6	GVSVF	18.98	60%	A0A0D5BEZ8|A0A0D5BEZ8_9MAGN
7	LXXF	18.62	75%	A0A9E9IWK0|A0A9E9IWK0_9MAGN
8	KAPGAVA	12.66	71.4%	Q05987|RBL_CERJA
9	IXXF	12.56	100%	A6YA81|A6YA81_9MAGN
10	LDNII	11.99	60%	A0A0D5BEZ8|A0A0D5BEZ8_9MAGN
11	ALIVI	10.68	100%	A0A1B1LMN9|A0A1B1LMN9_9MAGN
12	MNL	10.55	66%	Q9GI20|Q9GI20_9MAGN
13	PXXR	7.1	75%	A6YAD2|A6YAD2_9MAGN
14	MLE	5.44	60%	Q9TN17|Q9TN17_9MAGN

Note: X represents hidden amino acid residues

To identify the key peptide components in PSMPs that contribute to anti-aging activity, we first employed LC/MS/MS technology. Using PEAKS software, we conducted a database search to identify peptide sequences. For peptides that could not be successfully identified through the database, we applied de novo methods to identify their sequences. This dual approach aimed to maximize the identification of bioactive peptides with potential anti-aging effects. Based on the results from both identification strategies, we then established specific evaluation criteria to further refine and screen the obtained peptide sequences.

Literature suggests that the anti-aging activity of peptides is closely related to the hydrophobicity of their amino acid residues[16]. Therefore, we selected peptide sequences with a hydrophobic amino acid content > 60% as our screening criterion. Based on this threshold, we extracted 14 candidate peptidesfrom the identified database entries, as shown in Table 1. Further analysis revealed that these potential anti-aging peptides share a common feature: low molecular weight, typically composed of fewer than 7 amino acids. This finding implies that shorter peptides with smaller molecular weights may exhibit enhanced anti-aging activity, highlighting their potential as functional components in anti-aging formulations.

Table 2. PSMP Peptide Sequences with >60% Hydrophobic Amino Acid Content Screened from De Novo Explorer Data

Number	Peptide	ALC (%)	Length	Hydrophobic residues (%)	Area	Accession
1	VLRPPL	99.2	6	83	$7.91*10^7$	No report
2	VLRPLP	98.5	6	83	$7.91*10^7$	No report
3	VLRPPL	98.4	6	83	$7.91*10^7$	No report
4	NFAVLK	99	6	66.6	$4.07*10^7$	No report
5	YLLN	99.7	4	75	$3.39*10^7$	No report
6	RXXL	98.3	4	75	$2.76*10^7$	No report
7	LLVPT	98.9	5	80	$2.58*10^7$	No report
8	PVKLVR	99.8	6	66	$1.23*10^7$	No report
9	DFAVLK	99.7	6	66	$8.5*10^6$	No report
10	LAGL	95.9	4	75	$5*10^6$	No report

11	HWPW	99.8	4	80	$4.06*10^6$	No report
12	LWDHF	99.1	5	60	$3.99*10^6$	No report
13	DFAVLK	99.8	6	66	$3.2*10^6$	No report
14	PAPLL	96.9	5	100	$2.33*10^6$	No report
15	VVVSF	99.5	5	80	$1.84*10^6$	No report
16	LLAD	99.9	4	75	$1.74*10^6$	No report
17	RPPL	96.1	4	75	$1.51*10^6$	No report
18	FXXXA	98	5	80	$1.51*10^6$	No report
19	LXXXXV	98.7	6	66	$1.42*10^6$	No report
20	LXXXXF	100	6	80	$1.33*10^6$	No report

Note: X represents hidden amino acid residues

Table 3. Peptide Ranker Scores for 34 Selected Sequences from PSMPs

Number	Peptide	Score	Accession
1	LXR	0.93	report
2	YAL	0.43	report
3	SXF	0.90	report
4	RLI	0.41	report
5	IXXXL	0.80	report
6	GVSVF	0.35	report
7	LXXF	0.89	report
8	KAPGAVA	0.2	report
9	IXXF	0.89	report
10	LDNII	0.18	report
11	ALIVI	0.17	report
12	MNL	0.65	report
13	PXXR	0.97	report
14	MLE	0.27	report
15	VLRPPL	0.62	no report
16	VLRPLP	0.55	no report
17	VLRPPL	0.62	no report
18	NFAVLK	0.37	no report
19	YLLN	0.34	no report
20	RXXL	0.84	no report

21	LLVPT	0.18	no report
22	PVKLVR	0.14	no report
23	DFAVLK	0.4	no report
24	LAGL	0.48	no report
25	HXXW	0.98	no report
26	LXXXF	0.93	no report
27	DFAVLK	0.37	no report
28	PXXXL	0.83	no report
29	VVVSF	0.13	no report
30	LLAD	0.2	no report
31	RPPL	0.84	no report
32	FLAGA	0.61	no report
33	LRPGVV	0.17	no report
34	LLADAF	0.52	no report

Note: X represents hidden amino acid residues

In addition, we used De Novo Explorer software to perform de novo sequencing on the tandem mass spectrometry (MS/MS) data of the peptides. This method does not rely on protein database matching, allowing us to obtain a more comprehensive set of candidate peptide sequences. To improve the reliability of screening, we established multiple evaluation criteria, such as: peak area (signal intensity), sequence length (<7 amino acids), average local confidence (>95%) and Proportion of hydrophobic amino acids (>60%). As shown in Table 2, we identified 20 candidate peptides with potential anti-aging activity. By integrating the results of both identification methods, we obtained a total of 34 peptide sequences. Finally, we applied Peptide Ranker to score these peptides and found that 10 peptides had scores $>$ 0.8, as shown in Table 4. In the next step, we employed molecular docking to dock these 34 peptides with MMP-1 and elastase, aiming to identify key bioactive peptides that could play an effective role. This process will be evaluated by combining the results of molecular docking and the Peptide Ranker screening.

Molecular Docking

Table 4. Molecular Docking Binding Energies of 34 Potential Anti-Aging Peptides (PSMPs) with MMP-1 and Elastase

Number	Peptide	MMP-1: ΔG(kcal/mol)	Elastase: ΔG(kcal/mol)	Accession
1	LXR	-7.29	-5.98	report
2	YAL	-7.48	-5.40	report
3	SXF	-6.78	-5.99	report
4	RLI	-6.12	-4.67	report
5	IXXXL	-7.42	-5.21	report
6	GVSVF	-6.03	-4.85	report
7	LXXF	-6.92	-6.00	report
8	KAPGAVA	-5.72	-4.01	report
9	IXXF	-7.43	-6.37	report
10	LDNII	-4.70	-4.85	report
11	ALIVI	-4.89	-3.87	report
12	MNL	-5.85	-4.47	report
13	PXXR	-7.37	-6.09	report
14	MLE	-5.35	-4.45	report
15	VLRPPL	-5.25	-4.63	no report
16	VLRPLP	-5.36	-4.02	no report
17	VLRPPL	-5.25	-4.63	no report
18	NFAVLK	-5.8	-4.84	no report
19	YLLN	-5.51	-5.05	no report
20	RXXL	-8.34	-6.16	no report
21	LLVPT	-6.00	-5.02	no report
22	PVKLVR	-4.75	-4.07	no report
23	DFAVLK	-5.90	-4.23	no report
24	LAGL	-6.31	-4.44	no report
25	HXXW	-9.58	-7.06	no report
26	LXXXF	-8.26	-6.59	no report
27	DFAVLK	-5.90	-4.23	no report
28	PXXXL	-8.58	-6.16	no report
29	VVVSF	-5.17	-4.34	no report

30	LLAD	-5.67	-4.32	no report
31	RPPL	-8.17	-6.16	no report
32	FLAGA	-7.49	-4.36	no report
33	LRPGVV	-6.49	-4.31	no report
34	LLADAF	-5.92	-4.48	no report

Note: X represents hidden amino acid residues

Table 5. Ten Potential Anti-Aging Peptides (PSMPs) Identified through Dual Screening

Number	Peptide	Score	MMP-1: ΔG(kcal/mol)	Elastase: ΔG(kcal/mol)
1	LXR	0.93	-7.29	-5.98
2	SXF	0.90	-6.78	-5.99
3	IXXXL	0.8	-7.42	-5.21
4	LXXF	0.89	-6.92	-6.00
5	IXXF	0.89	-7.43	-6.37
6	PXXR	0.97	-7.37	-6.09
7	RXXL	0.84	-8.34	-6.16
8	HXXW	0.98	-9.58	-7.06
9	LXXXF	0.93	-8.26	-6.59
10	PXXXL	0.83	-8.58	-6.16

Note: X represents hidden amino acid residues

According to the molecular docking results shown in Table 4, 13 out of the 34 candidate peptides exhibited binding energies (ΔG) with MMP-1 and elastase below -5 kcal/mol. Among them, the binding energies with MMP-1 were particularly notable. This high-affinity interaction suggests that these peptides can effectively inhibit the activities of MMP-1 and elastase, thereby reducing the degradation of collagen and elastin, and exerting significant anti-aging effects. Based on the screening criterion of Peptide Ranker scores > 0.8, a total of ten peptides with potential anti-aging effects were identified, as listed in Table 5. These findings provide a theoretical foundation for considering these peptides as key bioactive components among the PSMPs with anti-aging properties.

4. Conclusion

The results of this study demonstrate that the bioenzymatically hydrolyzed peony seed meal peptides (PSMPs) we developed can exert multiple anti-oxidative (DPPH· and $ABTS^{+}$· scavenging) and anti-photoaging effects by modulating two inflammation- and aging-related pathways: NF-κB/NRF2 and NF-κB/AMPK. Notably, PSMPs exhibited superior inhibitory effects on MMP-1 and MMP-3 even at concentrations lower than those of the positive control group (VC + VE). Furthermore, through a combination of LC/MS/MS analysis, De Novo sequencing with custom peptide selection criteria, and dual screening via Peptide Ranker and molecular docking, we ultimately identified ten core peptide sequences with potential anti-aging effects. This study provides strong support for the application of peony seed meal-derived peptides as a natural anti-aging ingredient in skin care and anti-aging fields.

Reference

1. Zou, R., J. Xu, Z. Guo, Z. Wang, Z. Huang, L. Wang and L. Jiang. "Exploring sustainable sources and modification techniques of plant-based alternative proteins for high internal phase emulsion systems: From camellia oleifera seed meal, copra meal, and soybean meal." *Food Hydrocolloids* 166 (2025): 10.1016/j.foodhyd.2025.111256.

2. Tu, Y., R. An, H. Gu, N. Li, H. Yan, H.-Y. Liu and L. He. "The water extracts from the oil cakes of prinsepia utilis repair the epidermal barrier via up-regulating corneocyte envelope-proteins, lipid synthases, and tight junction proteins." Journal of Ethnopharmacology 330 (2024): 10.1016/j.jep.2024.118194.

3. Deng, R., J. Gao, J. Yi and P. Liu. "Peony seeds oil by-products: Chemistry and bioactivity." *Industrial Crops and Products* 187 (2022): 10.1016/j.indcrop.2022.115333.

4. Huang, J.-j., H.-l. Li, G.-q. Xiong, J. Cai, T. Liao and X.-y. Zu. "Extraction, identification and anti-photoaging activity evaluation of collagen peptides from silver carp (*hypophthalmichthys molitrix*) skin." *Lwt* 173 (2023): 10.1016/j.lwt.2022.114384.

5. Jia, D., G. Liao, B. Ye, M. Zhong, C. Huang and X. Xu. "Changes in fruit quality, phenolic compounds, and antioxidant activity of kiwifruit (*actinidia eriantha*) during on-vine ripening." *Lwt* 206 (2024): 10.1016/j.lwt.2024.116564.

6. Liu, Q., M. Xie, X. Li, Y. Song, Y. Wang, P. Hong and C. Zhou. "Development of curcumin-loaded hyaluronic acid complexes for curcumin intestinal delivery: Preparation, characterization, antioxidant, and in vitro digestive properties." *Lwt* 214 (2024): 10.1016/j.lwt.2024.117164.

7. Duan, Y., D. Deng, X. Yang, L. Zhang, X. Ma, L. He, G. Ma, S. Li and H. Li. "Bovine liver hydrolysates based on six proteases: Physicochemical properties, emulsification characteristics, antioxidant capacity assessment, and peptide identification." *Lwt* 208 (2024): 10.1016/j.lwt.2024.116718.

8. Yousuf, T., R. Akter, J. Ahmed, S. Mazumdar, D. Talukder, N. C. Nandi and M. Nurulamin. "Evaluation of acute oral toxicity, cytotoxicity, antidepressant and antioxidant activities of japanese mint (*mentha arvensis l.*) oil." *Phytomedicine Plus* 1 (2021): 10.1016/j.phyplu.2021.100140.

9. Hong, M., Y. Gui, J. Xu, X. Zhao, C. Jiang, J. Zhao, X. Xin, D. Liu, X. Tang, R. Tang*, et al.* "Palmitoyl copper peptide and acetyl tyrosine complex enhances melanin production in both a375 and b16 cell lines." *Biochemical and Biophysical Research Communications* 742 (2025): 10.1016/j.bbrc.2024.151060.

10. Wang, L., Z. Li, X. Fan, T. Zhang, H. Wang and K. Ye. "Novel antioxidant peptides from bovine blood: Purification, identification and mechanism of action." *Lwt* 205 (2024): 10.1016/j.lwt.2024.116499.

11. Lang, Y., N. Gao, Z. Zang, X. Meng, Y. Lin, S. Yang, Y. Yang, Z. Jin and B. Li. "Classification and antioxidant assays of polyphenols: A review." *Journal of Future Foods* 4 (2024): 193-204. 10.1016/j.jfutfo.2023.07.002.

12. Lu, Y., G. Pan, Z. Wei, Y. Li and X. Pan. "Role of fibroblast autophagy and proliferation in skin anti-aging." *Experimental Gerontology* 196 (2024): 10.1016/j.exger.2024.112559.

13. Maya-Cano, D. A., S. Arango-Varela and G. A. Santa-Gonzalez. "Phenolic compounds of blueberries (*vaccinium spp*) as a protective strategy against skin cell damage induced by ros: A review of antioxidant potential and antiproliferative capacity." *Heliyon* 7 (2021): 10.1016/j.heliyon.2021.e06297.

14. Xu, S., X. Sun, Z. Zhu, Y. Xin, C. Chen and J. Luo. "The extract of buds of chrysanthemum morifolium ramat alleviated uvb-induced skin photoaging by regulating mapk and nrf2/are pathways." *Journal of Ethnopharmacology* 332 (2024): 10.1016/j.jep.2024.118352.

15. Wang, T., Y. Wang, L. Liu, Z. Jiang, X. Li, R. Tong, J. He and J. Shi. "Research progress on sirtuins family members and cell senescence." *European Journal of Medicinal Chemistry* 193 (2020): 10.1016/j.ejmech.2020.112207.

16. Fan, X., Y. Han, Y. Sun, T. Zhang, M. Tu, L. Du and D. Pan. "Preparation and characterization of duck liver-derived antioxidant peptides based on lc-ms/ms, molecular docking, and machine learning." *Lwt* 175 (2023): 10.1016/j.lwt.2023.114479.